


Modeling the spin-Peierls transition of spin- $\frac{1}{2}$ chains with correlated states: J_1 - J_2 model, CuGeO₃, and TTF-CuS₄C₄(CF₃)₄

Sudip Kumar Saha ¹, Monalisa Singh Roy,¹ Manoranjan Kumar ^{1,*} and Zoltán G. Soos ^{2,†}

¹*S. N. Bose National Centre for Basic Sciences, Block JD, Sector III, Salt Lake, Kolkata 700106, India*

²*Department of Chemistry, Princeton University, Princeton, New Jersey 08544, USA*

 (Received 15 November 2019; revised manuscript received 7 January 2020; accepted 17 January 2020; published 7 February 2020)

The spin-Peierls transition at T_{SP} of spin- $\frac{1}{2}$ chains with isotropic exchange interactions has previously been modeled as correlated for $T > T_{\text{SP}}$ and mean field for $T < T_{\text{SP}}$. We use correlated states throughout in the J_1 - J_2 model with antiferromagnetic exchange J_1 and $J_2 = \alpha J_1$ between first and second neighbors, respectively, and variable frustration $0 \leq \alpha \leq 0.50$. The thermodynamic limit is reached at high T by exact diagonalization of short chains and at low T by density matrix renormalization group calculations of progressively longer chains. In contrast to mean field results, correlated states of 1D models with linear spin-phonon coupling and a harmonic adiabatic lattice provide an internally consistent description in which the parameter T_{SP} yields both the stiffness and the lattice dimerization $\delta(T)$. The relation between T_{SP} and $\Delta(\delta, \alpha)$, the $T = 0$ gap induced by dimerization, depends strongly on α and deviates from the BCS gap relation that holds in uncorrelated spin chains. Correlated states account quantitatively for the magnetic susceptibility of TTF-CuS₄C₄(CF₃)₄ crystals ($J_1 = 79$ K, $\alpha = 0$, $T_{\text{SP}} = 12$ K) and CuGeO₃ crystals ($J_1 = 160$ K, $\alpha = 0.35$, $T_{\text{SP}} = 14$ K). The same parameters describe the specific heat anomaly of CuGeO₃ and inelastic neutron scattering. Modeling the spin-Peierls transition with correlated states exploits the fact that $\delta(0)$ limits the range of spin correlations at $T = 0$ while $T > 0$ limits the range at $\delta = 0$.

DOI: [10.1103/PhysRevB.101.054411](https://doi.org/10.1103/PhysRevB.101.054411)

I. INTRODUCTION

Jacobs *et al.* [1] identified the spin-Peierls transition at $T_{\text{SP}} = 12$ K in the organic crystal TTF-CuS₄C₄(CF₃)₄. The spin- $\frac{1}{2}$ chain at $T > T_{\text{SP}}$ has equally spaced cation radicals TTF⁺ and is dimerized at lower T . They analyzed the magnetic susceptibility $\chi(T)$ using the linear Heisenberg antiferromagnet with equal exchange J_1 to both neighbors for $T > T_{\text{SP}}$ and alternating exchange $J_1(1 \pm \delta(T))$ in the dimerized phase. The T dependence of $\delta(T)$ followed the BCS gap equation of superconductors. Subsequently, Hase *et al.* [2] identified the inorganic spin-Peierls crystal CuGeO₃ with $T_{\text{SP}} = 14$ K based on spin- $\frac{1}{2}$ chains of Cu(II) ions. The magnetic susceptibility at $T > T_{\text{SP}}$ indicated [3] exchange $J_2 = \alpha J_1$ with $\alpha = 0.35$ between second neighbors in addition to J_1 . However, $\delta(T)$ did not follow BCS and extensive CuGeO₃ studies have been inconclusive [4] with respect to frustration α . These prototypical spin-Peierls (SP) crystals have been analyzed with correlated states for $T > T_{\text{SP}}$ but only as uncorrelated or mean field for $T < T_{\text{SP}}$.

Spin- $\frac{1}{2}$ chains have been long studied theoretically as simple 1D systems with two states, α and β , per site. The linear Heisenberg antiferromagnet (HAF) is the $\alpha = 0$ limit of the J_1 - J_2 model, Eq. (4) below. The HAF may well be the best characterized many-body system, and the J_1 - J_2 model also has an extensive literature.

The electronic problem for SP transitions is to obtain the thermodynamic limit of the free energy per site $A(T, \delta)$ at temperature T and dimerization δ . In reduced ($J_1 = 1$) units, we have

$$A(T, \delta) = -T \ln Q(T, \delta). \quad (1)$$

The thermodynamic limit is known for free fermions but not for correlated systems such as the HAF or the J_1 - J_2 model. SP modeling has consequently been approximate and subject to revision due to computational advances. In particular, we show below that $\delta(T)$ for the HAF does *not* follow BCS.

We model both transitions with a recent method that combines exact diagonalization (ED) of short chains with density matrix renormalization group (DMRG) calculations of progressively longer chains [5]. The premise is that the full spectrum $\{E(\delta, N)\}$ of large systems is never needed. Since T limits the range of spin correlations, ED is sufficient once the system size exceeds the correlation length. Bonner-Fisher results [6] to $N = 12$ were used [1] for $\chi(T)$ of TTF⁺ chains at $T > T_{\text{SP}}$. ED to $N = 24$ is now accessible. DMRG for larger N yields the spectrum $\{E(\delta, N)\}$ up to some cutoff $E_C(\delta, N)$, thereby extending thermodynamics to lower T . The hybrid approach is particularly well suited for SP systems because dimerization opens a gap that limits spin correlations at $T = 0$.

The driving force for dimerization is the partial derivative $\partial A(T, \delta)/\partial \delta$ that is opposed by the lattice. The simplest lattice model is used in conventional approaches [7–9] to the Peierls or SP instability: The coupling is linear, the potential energy $\delta^2/2\epsilon_d$ per site is harmonic, and the stiffness $1/\epsilon_d$ is

*manoranjan.kumar@bose.res.in

†soos@princeton.edu

independent of T . The equilibrium dimerization is

$$\frac{\delta(T)}{\varepsilon_d} = - \left(\frac{\partial A(T, \delta)}{\partial \delta} \right)_{\delta(T)}. \quad (2)$$

At $T = 0$, $A(0, \delta) = E_0(\delta)$ is the ground-state energy per site. DMRG returns the derivative $E'_0(\delta, N)$ of large systems and the extrapolated limit $E'_0(\delta)$. Dimerization decreases and vanishes at T_{SP} , where $1/\varepsilon_d = -A''(T_{\text{SP}}, 0)$. In principle, the observed T_{SP} is the model parameter that specifies both the stiffness and $\delta(T)$. To emphasize the point, we refer to the equilibrium susceptibility as $\chi(T, T_{\text{SP}})$ over the entire range. Moreover, the driving force is a property of the electronic system that is balanced by whatever model is adopted for the lattice.

The equilibrium dimerization is explicitly known for free fermions; $\delta(T)$ for a half-filled tight-binding band is given by

$$\frac{1}{\varepsilon_d} = \frac{8}{\pi} \int_0^{\pi/2} dk \frac{\sin^2 k}{\varepsilon(k, \delta(T))} \tanh \frac{\varepsilon(k, \delta(T))}{2T},$$

$$\varepsilon(k, \delta) = 2\sqrt{\cos^2 k + \delta^2 \sin^2 k}. \quad (3)$$

The stiffness is half as large for spinless fermions, which corresponds to the XY spin- $\frac{1}{2}$ chain. The band gap opens as $2\varepsilon(\pi/2, \delta) = 4\delta$ and $\delta(0)$ goes as $\exp(-1/\varepsilon_d)$ in the weak-coupling limit. The spinless fermion representation of the HAF has interactions between first neighbors. The HAF is correlated. Although not exact, the HAF gap opens [10] as $\delta^{3/4}$ based on diverse numerical studies collected in Ref. [11]. The DMRG exponent in the range $0.001 \leq \delta \leq 0.10$ is [12] 0.7475 ± 0.0075 .

To illustrate correlations and frustration, we show in Fig. 1 the dimerization of spin chains with $T_{\text{SP}} = 0.09$ (or $0.09J_1$). The fermion curve is Eq. (3) with $4/\pi$ instead of $8/\pi$; the band gap $4\delta(0) = 3.55T_{\text{SP}}$ is within 1% of the BCS gap relation. The other curves are $A'(T, \delta, N)$ for J_1 - J_2 models with $N = 32$ in Eq. (4), periodic boundary conditions, and $\alpha = 0$ (HAF), 0.35, and 0.50. The fermion $\delta(T)$ scaled by $1/1.59$ is the dashed line through the HAF points; the scaled T dependence is nearly BCS. The stiffness increases by an order of magnitude from the HAF to MG while $\delta(0)$ decreases by a factor of four and $\delta(T)$ clearly deviates from free fermions.

We analyze SP transitions of the J_1 - J_2 model with frustration $0 \leq \alpha \leq 0.50$. Under some conditions, numerical advances have made accessible the thermodynamic limit of correlated states of 1D systems. The influential but approximate HAF analysis [1, 13] of TTF-CuS₄C₄(CF₃)₄ was widely thought to apply to the larger data set made possible by sizable CuGeO₃ crystals. But CuGeO₃ turned out to be different and has largely resisted modeling. Correlated states provide a consistent description of both SP transitions.

The paper is organized as follows. Section II presents the calculation of $A'(T, \delta)$ in J_1 - J_2 models with frustration α and the criterion for the thermodynamic limit. We model in Sec. III the magnetic susceptibility $\chi(T, T_{\text{SP}})$ of TTF-CuS₄C₄(CF₃)₄ with two parameters, $J_1 = 79$ K and $T_{\text{SP}} = 12$ K. The CuGeO₃ parameters $J_1 = 160$ K, $\alpha = 0.35$, and $T_{\text{SP}} = 14$ K account for both $\chi(T, T_{\text{SP}})$ and the specific heat anomaly, $C(T, T_{\text{SP}})$. In Sec. IV we discuss the CuGeO₃ excitations probed by inelastic neutron scattering, not modeled previously, that give an independent determination of J_1 . We also study the

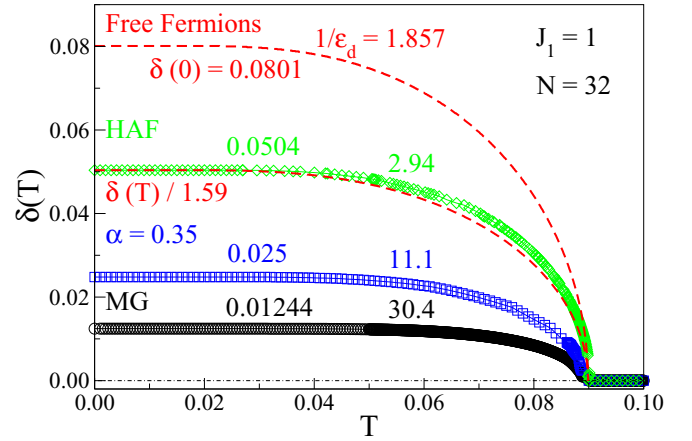


FIG. 1. Equilibrium dimerization $\delta(T)$ of spin chains with $T_{\text{SP}} = 0.09$ leading to stiffness $1/\varepsilon_d$ and $\delta(0)$ in Eq. (2). The exact free fermion curve is Eq. (3) with $4/\pi$ instead of $8/\pi$. The HAF ($\alpha = 0$), $\alpha = 0.35$, and MG ($\alpha = 0.50$) curves are based on Eq. (4) with $N = 32$ spins. The HAF dimerization is close to the fermion $\delta(T)/1.59$. Note the large variation of $1/\varepsilon_d$ and $\delta(0)$ in chains with equal T_{SP} .

Majumdar-Ghosh (MG) point [14], $\alpha = 0.50$, where the exact ground state is known. Aspects and limitations of 1D models are mentioned in the discussion (Sec. V).

II. DIMERIZED J_1 - J_2 MODEL

The J_1 - J_2 model has isotropic exchange interactions $J_1, J_2 = \alpha J_1$ between first and second neighbors of a regular ($\delta = 0$) spin- $\frac{1}{2}$ chain. The dimerized model has alternating $J_1(1 \pm \delta)$ along the chain. We consider finite chains with $N = 4n$ spins, periodic boundary conditions, and $J_1 = 1$ as the unit of energy. The electronic Hamiltonian is

$$H(\delta, \alpha) = \sum_r [1 + \delta(-1)^r] \vec{S}_r \cdot \vec{S}_{r+1} + \alpha \sum_r \vec{S}_r \cdot \vec{S}_{r+2}. \quad (4)$$

The HAF is the special case $\alpha = \delta = 0$. The ground state of $H(0, \alpha)$ is nondegenerate for $0 \leq \alpha \leq \alpha_c = 0.2411$, the quantum critical point [15] that separates a gapless phase from the gapped dimer phase with a doubly degenerate ground state. The exact $\delta = 0$ ground state is known at $\alpha = 0.50$, the MG point [14], that marks the onset of an incommensurate phase. Finite δ breaks inversion symmetry at sites and increases the singlet-triplet gap $\Delta(\delta, \alpha)$ but does not change the length in systems with periodic boundary conditions. The analysis does not depend on the index α which is suppressed below.

We consider the equilibrium Eq. (2) with increasing system size to obtain the thermodynamic limit at finite T and then evaluate $\delta(T)$ in models with $T_{\text{SP}} > T$. The free energy per spin of finite chains is

$$A(T, \delta, N) = -TN^{-1} \ln Q(T, \delta, N). \quad (5)$$

The Boltzmann sum in $Q(T, \delta, N)$ is over the 2^N spin states with energies $E_r(\delta, N)$. Exact diagonalization (ED) yields the full spectrum of short chains. The equilibrium dimerization requires the partial derivative that we approximate as

$$A'(T, \delta, N) \approx \frac{A(T, \delta + \varepsilon, N) - A(T, \delta - \varepsilon, N)}{2\varepsilon}. \quad (6)$$

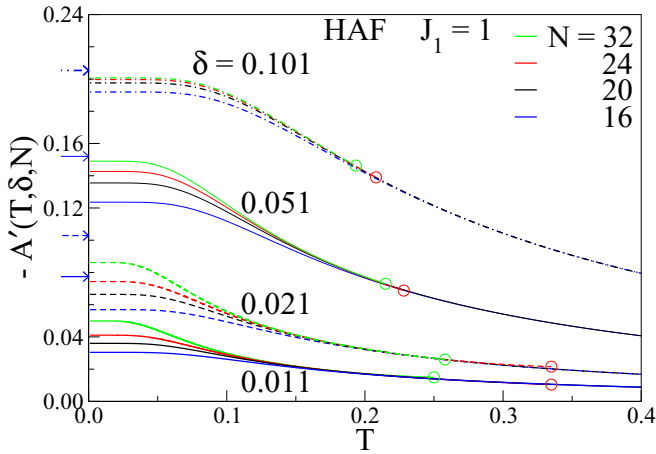


FIG. 2. Driving force for dimerization, $-A'(T, \delta, N)$, of HAF chains with N spins and $\alpha = 0$ in Eq. (4). $N = 16$ and 20 are exact. DMRG for $N = 24$ and 32 is shown up to $T'(\delta, N)$, shown as open circles, the maximum of $S_C(T, \delta, N)/T$ discussed in the text. Arrows at $T = 0$ are thermodynamic limits that increase with δ .

The numerator is accurate to three decimal places for $\varepsilon = 0.001$. We find that the size dependence of A' is considerably weaker than that of A , presumably due to cancellations in the numerator.

The hybrid ED/DMRG method [5] follows the size dependence of the quantity of interest, here the driving force $-A'(T, \delta, N)$. Since T reduces the range of spin correlations, ED up to $N = 24$ for $\delta = 0$ or $N = 20$ for $\delta > 0$ returns the thermodynamic limit at high T . DMRG with periodic boundary conditions [16] is then used to obtain the lowest few thousand states of larger systems. The spectrum $E_r(\delta, N) \leq E_C(\delta, N)$ up to a cutoff defines a truncated partition function $Q_C(T, \delta, N)$ and hence a truncated entropy per site, $S_C(T, \delta, N)$. Finite-size gaps reduce $S_C(T, \delta, N)$ compared to the actual entropy at low T while truncation reduces it at high T . Since $S_C(T, \delta, N)/T$ converges from below with increasing N , its maximum at $T'(\delta, N)$ is the best choice for a given cutoff $E_C(\delta, N)$. The cutoff is increased until $T'(\delta, N)$ is independent or almost independent of E_C . The thermodynamic limit of $A'(T', \delta)$ at $T'(\delta, N)$ is approximated by DMRG at system size N .

Figure 2 illustrates the T dependence of $-A'(T, \delta, N)$ of the HAF. As expected for any α , $-A'$ decreases with T and increases N to the thermodynamic limit. The $N = 16$ and 20 lines are exact. DMRG results for $N > 20$ extend to the points $T'(\delta, N)$, the maxima of $S_C(T, \delta, N)/T$ that are shown as open circles. Finite-size gaps are evident around $T \sim \delta \sim 0$, where $-A'(T, \delta, N)$ is constant. Arrows indicate the $T = 0$ intercepts, $-E'_0(\delta, N)$, that are obtained by extrapolation of ground-state DMRG calculations [12] at constant δ . Since δ opens a magnetic gap in the infinite chain, the size dependence decreases as seen at $\delta = 0.101$. Convergence to the thermodynamic limit is found by $T \sim 0.15$. The general criterion based on $T'(\delta, N)$ is evidently conservative for $A'(T, \delta, N)$, which is seen to converge at lower T .

The size dependence of $A'(T, \delta, N)$ in the dimer phase is shown in Fig. 3 for $\alpha = 0.35$ and 0.50 in Eq. (4). The MG ground states are the two Kekulé valence bond diagrams

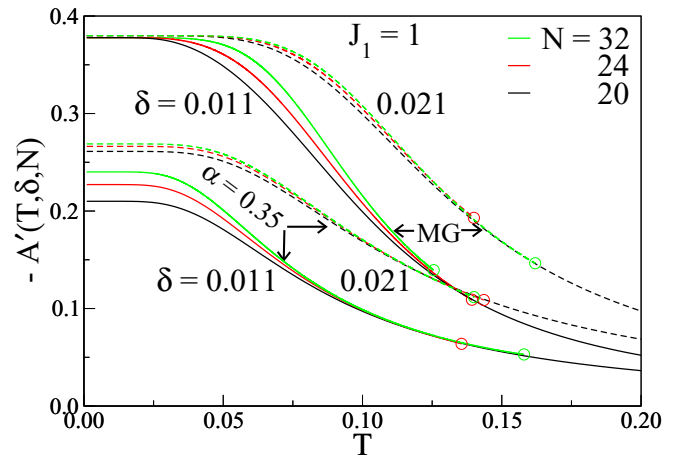


FIG. 3. Same as Fig. 2 for frustration $\alpha = 0.35$ and MG ($\alpha = 0.50$) in Eq. (4).

with singlet pairing either between all sites $2r, 2r - 1$ or all sites $2r, 2r + 1$. The energy per site is $-3/8$ for even N in Eq. (4) and $A'(0, \delta, N) = -3/8$ is exact [17] to order δ . The thermodynamic limit is reached by $T \sim 0.13$ for $\alpha = 0.50$. The size dependence at $\alpha = 0.35$ is intermediate. The ground state degenerates in the thermodynamic limit but not for finite N . The $-A'(0, 0, N)$ intercept decreases with N to $B(0.35) = 0.078$ in the thermodynamic limit, where $B(\alpha)$ is the amplitude of the bond order wave [18]. The size dependence again decreases with δ .

Figures 2 and 3 indicate how $A'(T, \delta, N)$ approaches the thermodynamic limit. The convergence depends on the model and the largest system N_m ,

$$A'(T, \delta, N_m) \rightarrow A'(T, \delta), \quad T > T'(\delta, N_m). \quad (7)$$

$T'(\delta, N_m)$ is the maximum of $S_C(\delta, T, N_m)/T$ of the largest system considered. We have performed DMRG calculations up to $N \sim 100$, but smaller N may be sufficient and convergence at $\delta = 0$ typically also holds for $\delta > 0$. The system size is eventually limited [5] by the numerical accuracy of the dense energy spectrum, which is of course model dependent. Although the mathematically interesting $A'(T, 0)$ at $T \sim 0$ is out of reach, modeling SP transitions merely requires $T_{\text{SP}} > T'(0, N_m)$. The equilibrium Eq. (2) then gives $\delta(T)$ in the thermodynamic limit.

Figure 4 shows $A'(T, \delta, N)$ vs δ for models with $N = 32$ and $\alpha = 0$ (HAF) or 0.50 (MG). These curves are the lower and upper bounds of $-A'(T, \delta, N)$ for J_1 - J_2 models with $0 \leq \alpha \leq 0.50$. The $\delta = 0$ intercept at $T = 0$ decreases from $3/8$ at $\alpha = 0.50$ to zero at $\alpha_c = 0.2411$, where [12,19] $E'_0(\delta) = -0.62\delta^{0.33}$. The HAF result [12] is $E'_0(\delta) = 0.56\delta^{0.44}$. The graphical solutions $\delta(T, \alpha)$ of Eq. (2) are the intersections in Fig. 4 of $A'(T, \delta, N)$ with dashed lines δ/ε_d at the indicated stiffness. The chains are unconditionally unstable for finite ε_d since $E'_0(\delta)$ is finite at $\delta = 0$ for $\alpha > \alpha_c$ while $E''_0(\delta)$ diverges at $\delta = 0$ for $\alpha < \alpha_c$. The $E'_0(\delta)$ cusp at $\delta = 0$ in the dimer phase leads to the flatter two $\delta(T)$ curves [17] in Fig. 1.

We conclude that the thermodynamic limit $A'(T, \delta)$ can be reached in finite chains at $T = 0$ when $\delta > 0$ or at $\delta = 0$ when $T > 0$. The $T > T_{\text{SP}}$ range is more accessible numerically

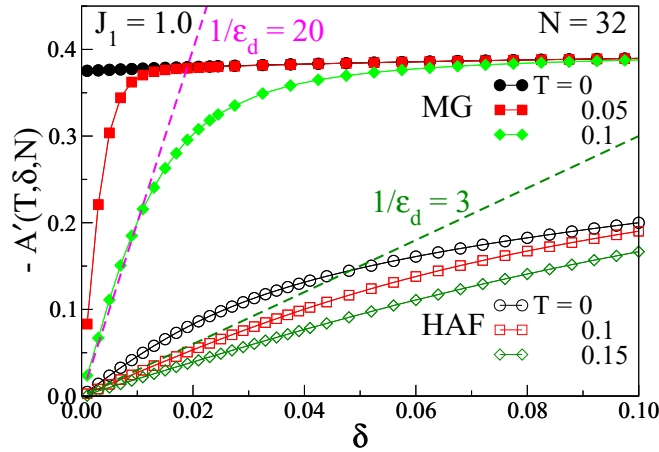


FIG. 4. The driving force $-A'(T, \delta, N)$ at reduced T of MG and HAF chains with $N = 32$ and $\alpha = 0.50$ and 0 in Eq. (4). The dashed lines are δ/ϵ_d and crossing points are solutions $\delta(T)$ to Eq. (2). The HAF and MG curves are lower and upper bounds for frustration $0 \leq \alpha \leq 0.50$.

for large T_{SP}/J_1 that in turn generates large $\delta(0)$. The relation between T_{SP} and $\delta(0)$ is strongly model dependent as seen in Fig. 1.

III. MAGNETIC SUSCEPTIBILITY AND SPECIFIC HEAT

A sudden decrease of the molar magnetic susceptibility $\chi(T)$ at $T < T_{SP}$ is a direct manifestation of an SP transition. Figure 5 shows published data for [1] TTF-CuS₄C₄(CF₃)₄ and [2,20] CuGeO₃ on a log scale that emphasizes low T . The excellent TTF⁺ fit shown in Fig. 5 of Ref. [1] or Fig. 10 of Ref. [13] is based on the HAF with $J_1 = 77$ K and $g = 1.97$ for $T > T_{SP} = 12$ K. The g value is within the range given by electron spin resonance (ESR) with the applied magnetic field along the c axis. The $T \sim 0$ limit is shown as slightly positive ($\sim 0.08 \times 10^{-3}$ emu/mol).

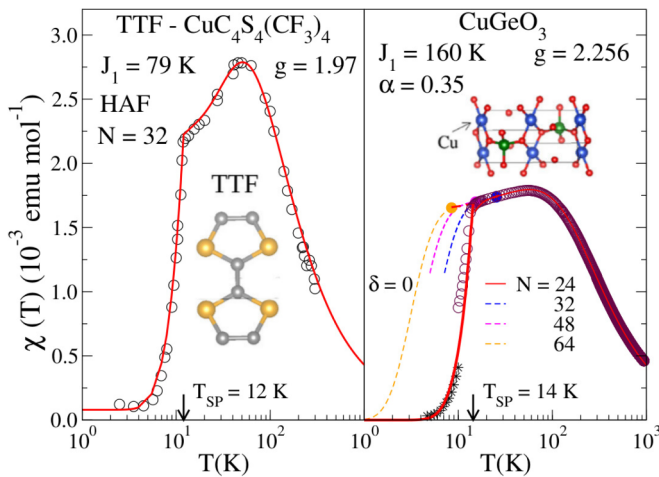


FIG. 5. Absolute molar magnetic susceptibility: TTF-CuS₄C₄(CF₃)₄ data from Fig. 5 of Ref. [1] or Fig. 10 of Ref. [13]; CuGeO₃ data from Ref. [2] to 10 K and Ref. [20] for $T > 10$ K. Fits are discussed in the text. The $\delta = 0$ lines are DMRG up to $T'(0, N)$ shown as filled circles.

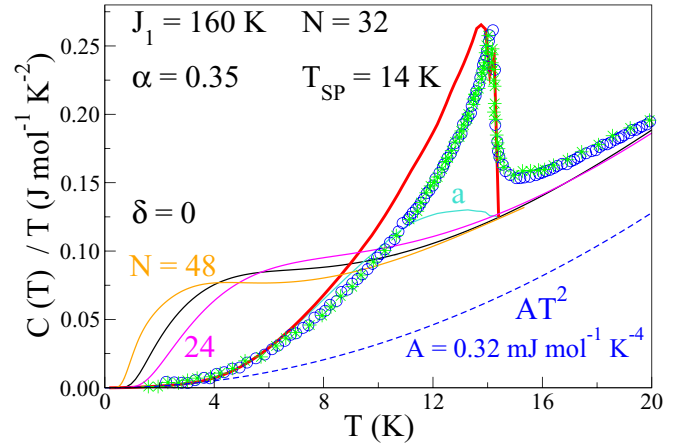


FIG. 6. Molar specific heat $C(T)$ of CuGeO₃ shown as the entropy derivative $S' = C/T$: Blue circles from Ref. [24], green stars and A from Ref. [25]. The calculated $C(T, 0)/T$ curves are ED for $N = 24$, DMRG for $N = 32$ and 48 . The equilibrium $C(T, T_{SP})/T$ is the bold red line, Eq. (8), whose first term is labeled “a”.

We included this T -independent contribution in the correlated fit shown with $J_1 = 79$ K, $T_{SP} = 12$ K, and $g = 1.97$. The $\delta = 0$ curve above T_{SP} is ED for $N = 24$ and DMRG for $N = 32$ with $\alpha = 0$ in Eq. (4). In the dimerized phase, we calculated $\chi(T, T_{SP})$ for $N = 32$ at the equilibrium $\delta(T)$ given by Eq. (2). The correlated fit is equally quantitative. It has one fewer parameter and is internally consistent: T_{SP} and J_1 determine both the stiffness $1/\epsilon_d = 1.96$ and $\delta(0) = 0.103$. The previous $\chi(T, \delta(T))$ was based [1] on a mean field $\delta(T)$ for the T dependence and required an adjustable $\delta(0) = 0.126$ that, as noted, [1] leads to $T_{SP} = 9$ rather than 12 K.

The range of spin correlations is reduced at low T by substantial dimerization $\delta(0) = 0.10$. The thermodynamic limit is reached in relatively short chains that are now amenable to quantitative analysis. Correlated states clarify the SP transition of TTF-CuS₄C₄(CF₃)₄. Contrary to long held expectations, the HAF dimerization $\delta(T)$ does *not* follow free fermions or BCS.

The $\chi(T)$ data for CuGeO₃ are from Ref. [2] up to 10 K ($T_{SP} = 14$ K) and from Ref. [20] from 10 to 950 K ($T_{SP} = 14.3$ K), kindly provided in digital form by Professor Lorenz. There is a mismatch at 10 K. The range (~ 0.5 K) of reported T_{SP} reflect variations of growth conditions that are discussed in Ref. [21]. We retained the previous parameters [20] based on ED for $N = 18$ and the $\chi(T)$ maximum at $T = 56$ K: $J_1 = 160$ K, frustration $\alpha = 0.35$ in Eq. (4), and $g = 2.256$ from ESR. The $\delta = 0$ fit is quantitative for $T > T_{SP} = 14$ K ($0.09J_1$). The points $T'(N)$ on the $\delta = 0$ curve are the $S_C(T, 0, N)/T$ maxima of truncated calculations at system size N . The resulting $\chi(T, T_{SP})$ for $T < T_{SP}$ is consistent with the available data and corresponds to $\delta(0) = 0.025$. We extend [20] or improve [22,23] previous $T > T_{SP}$ fits.

Sizable single crystals of CuGeO₃ made possible other measurements. The specific heat $C(T)$ to 20 K is shown in Fig. 6 as the entropy derivative $S' = C/T$ in Refs. [24,25]. The dashed line is the reported lattice (Debye) contribution [25], AT^2 , with $A = 0.32$ mJ/mol K⁴. The specific heat has not been modeled aside from the initial exponential increase

with T . The anomaly is sharper and better resolved than in small TTF-CuS₄C₄(CF₃)₄ crystals [26].

The equilibrium $C(T, T_{\text{SP}})$ has two contributions [17] below T_{SP} ,

$$C(T, T_{\text{SP}}) = C(T, \delta(T)) + \frac{\partial \delta}{\partial T} \left[\left(\frac{\partial E(T, \delta)}{\partial \delta} \right)_T + \frac{\delta(T)}{\varepsilon_d} \right]. \quad (8)$$

$E(T, \delta)$ is the internal energy per site, $-\partial \ln Q(\beta, \delta)/\partial \beta$ with $\beta = 1/k_B T$. The first term is evaluated at $\delta(T)$ along the equilibrium $\alpha = 0.35$ line in Fig. 1, which can be fitted quantitatively as

$$\frac{\delta(T)}{\delta(0)} = \left[1 - \left(\frac{T}{T_{\text{SP}}} \right)^a \right]^b, \quad T \leq T_{\text{SP}}, \quad (9)$$

with $a = 5.29$ and $b = 0.689$. We used Eq. (9) to evaluate $\partial \delta/\partial T$. The calculated $C(T, T_{\text{SP}})/T$ is the bold red line shown in Fig. 6. The low- T behavior of $\delta = 0$ chains is a finite-size effect. Since gaps initially decrease $C(T, N)/T$, entropy conservation requires increased $C(T, N)/T$ before converging from above to the thermodynamic limit. The $N = 48$ and 24 gaps are smaller and larger, respectively, than $N = 32$, which is in the thermodynamic limit for $T > 12$ K.

The $C(T, \delta(T))/T$ part of Eq. (8) is the curve labeled ‘‘a’’ in Fig. 6. The $\partial \delta(T)/\partial T$ derivative is mainly responsible for the sharp anomaly. The area under $C(T, T_{\text{SP}})/T$ up to T_{SP} is within 5% of the accurately known $\delta = 0$ area. The adiabatic and mean field approximations for the lattice enforce $\delta = 0$ for $T > T_{\text{SP}}$; this general problem for any transition has long been recognized. The agreement between theory and experiment by 20 K implies equal area under the measured, dimerized, and $\delta = 0$ curves in Fig. 6. Lattice fluctuations observed above T_{SP} must be offset by reduced C/T below T_{SP} . Overall, the anomaly is fitted rather well considering these approximations.

IV. INELASTIC NEUTRON SCATTERING

Dimerization opens a gap $\Delta(\delta, \alpha)$ in gapless spin chains or increases the gap in gapped chains. The gap is from the singlet ($S = 0$) ground state to the lowest energy triplet ($S = 1$). The opening of the HAF gap [10,11] $\Delta(\delta, 0)$ or of $\Delta(\delta, \alpha_c)$ at the critical point [12,19] has been extensively discussed using field theory and numerical methods; $\Delta(0, \alpha)$ is finite in the dimer phase, exponentially small just above α_c , and substantial at $\alpha = 0.50$. We obtained the thermodynamic limit of gaps in Fig. 7 by extrapolation of DMRG calculations up to $N = 96$. As expected, size convergence is rapid for $\delta > 0.01$. The gap opens as

$$\Delta(\delta, \alpha) = \Delta(\alpha) + D\delta^\gamma, \quad (10)$$

with $\Delta = 0.0053$, $D = 2.03$, and $\gamma = 0.585$ for $\alpha = 0.35$. The T dependence is given by $\delta(T)$. The large MG gap is $\Delta(0, 0.5) = 0.233$.

Inelastic neutron scattering (INS) at $T = 0$ is exclusively to triplets in models with isotropic exchange. Figure 8 shows the scaled gap $\Delta(T)/\Delta(0)$ vs T/T_{SP} . The solid line is the calculated $\Delta(\delta(T), 0.35)$ in Eq. (10) with $\delta(T)$ in Eq. (9) or the $\alpha = 0.35$ curve in Fig. 1. The gap $\Delta J_1 = 0.85$ K is almost an order of magnitude below INS resolution and scales

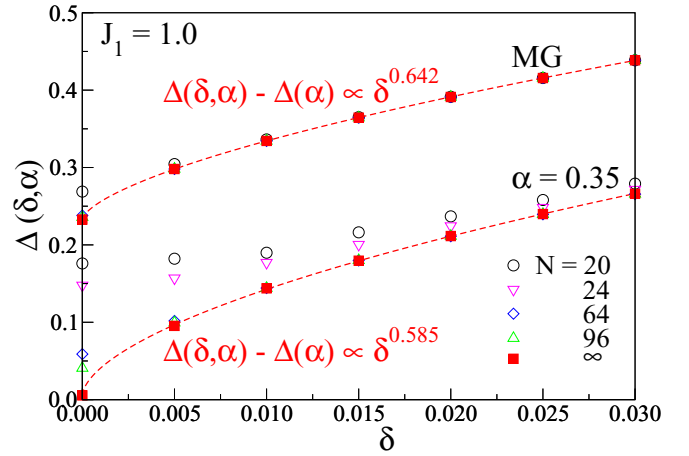


FIG. 7. Scaled singlet-triplet gap $\Delta(T, \delta, N)$ at $T = 0$ of N -spin chains in Eq. (4) with dimerization δ and frustration $\alpha = 0.35$ and 0.50. The lines are $1/N$ extrapolations of DMRG to $N = 96$. Note the rapid convergence at the MG point.

to 0.022 for $T > T_{\text{SP}}$ and $\delta(0) = 0.025$. The dashed line is the gap ratio $\delta(T)/\delta(0)$ for free fermions in Fig. 1. INS studies of CuGeO₃ crystals in Refs. [27–30] have reported the T dependence of the singlet-triplet gap $\Delta(T)$. (The organic crystals are unsuitably small [30].) Large deviations from the free fermions or BCS were unexpected and unexplained. Correlated states are consistent with these data, and how quantitatively remains to be seen.

The calculation of the INS spectrum is straightforward in finite systems with periodic boundary conditions. Triplets $|T_n(q)\rangle$ at $E_n(q)$ relative to the singlet ground state $|G\rangle$ are required. At $T = 0$, the INS intensity $M_n(q)$ for energy transfer $\omega = E_n(q)$ and momentum transfer q is [31]

$$M_n(q) = 2\pi |(T_n(q)|S_q^z|G)|^2, \quad S_q^z = (4n)^{-\frac{1}{2}} \sum_r e^{iqr} S_r^z. \quad (11)$$

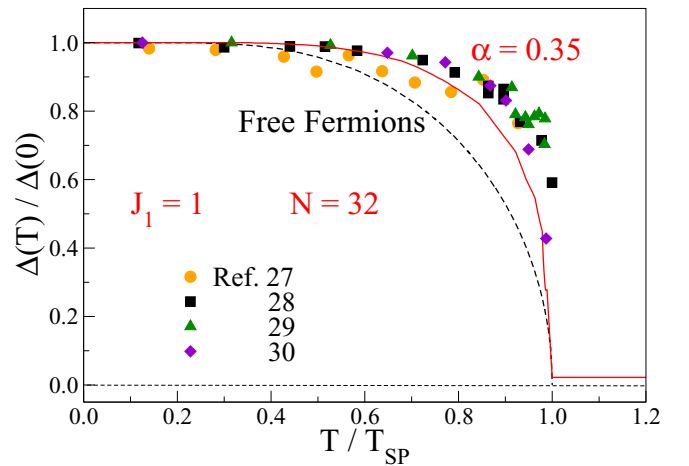


FIG. 8. Scaled singlet-triplet gap $\Delta(T)/\Delta(0)$ vs T/T_{SP} . The solid line is $\Delta(\delta(T), \alpha)/\Delta(\delta(0), \alpha)$ with $\alpha = 0.35$ in Eq. (10); the dashed line is $\delta(T)/\delta(0)$ for free fermions in Fig. 1. The symbols are inelastic neutron data from Refs. [27–30].

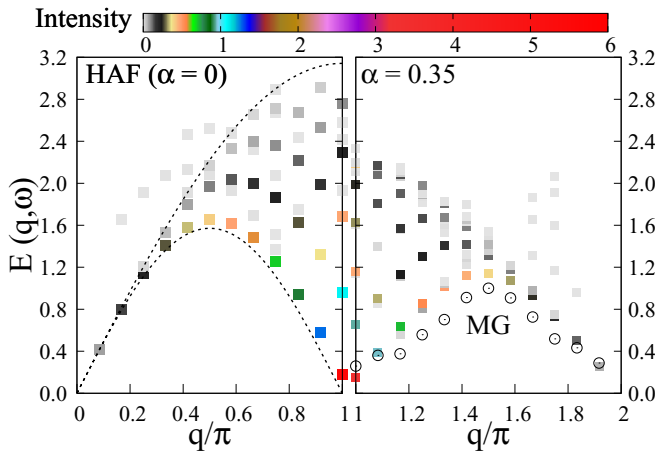


FIG. 9. Exact triplet excitations $E_n(q)$ at wave vector q in 24-spin chains: Left panel, $\alpha = 0$ (HAF); right panel, $\alpha = 0.35$. The color coding is the intensity $M_n(q) > 0.001$ in Eq. (11). The lowest triplets $E_1(q)$ for $\alpha = 0.50$ (MG) are the open circles on the right. The dashed lines are the spinon boundaries, Eq. (13).

The x or y components of S_q also yield $M_n(q)$. The lowest triplet of $H(\delta, \alpha)$ is $E_1(\pi) = \Delta(\delta, \alpha)$. The INS intensity at finite T is the thermal average [31] of Eq. (11) over excited states as well as $|G\rangle$. The static structure factor at $T = 0$ is given by ground-state spin correlation functions

$$S(q) = \langle G | S_{-q}^z S_q^z | G \rangle. \quad (12)$$

The total INS intensity per spin is $\pi/2$ for chains with a singlet ground state. The thermal average of $S(T, q)$ in Eq. (12) is far less tedious since it only requires the T dependence of $N/2$ correlation functions.

The Bethe ansatz [32] has provided the exact ground state of the HAF and the so-called class C states with $S > 0$ that can be solved exactly. Faddeev and Takhtajan [33] obtained the double-spinon continuum in the thermodynamic limits. The lower and upper boundaries at wave vector q are

$$\begin{aligned} \varepsilon_1(q) &= \frac{\pi}{2} \sin q, & 0 \leq q \leq \pi, \\ \varepsilon_2(q) &= \pi \sin \frac{q}{2}. \end{aligned} \quad (13)$$

Each state is fourfold degenerate, two $S = \frac{1}{2}$ spinons forming a triplet or a singlet. The boundaries up to $q = \pi$ are the dashed lines in the HAF panel of Fig. 9. The spectrum is symmetric about $q = \pi$. The singlet-triplet gap $\varepsilon_1(q)$ was found earlier by des Cloizeaux and Pearson [34].

The almost quantitative calculation of intensities $M_n(q)$ in the thermodynamic limit has recently been achieved [35]. Mourigal *et al.* [36] have confirmed theory in detail on a Cu(II) spin chain with $J_1 = 2.93$ K; the INS analysis in Fig. 1(d) of Ref. [36] was carried out at finite T using both two- and four-spinon calculations. $S(q, \omega)$ is continuous in the thermodynamic limit. Figure 1(d) is color coded according to intensity and impressive agreement between theory and experiment is shown, as in Fig. 9, side by side with $0 \leq q \leq \pi$ and $\pi \leq q \leq 2\pi$.

When total spin is conserved, a system of $N = 4n$ spins has $3(4n)! / [(2n-1)!(2n+2)!]$ triplets out of which only

$n(2n+1)$ are in class C [32] and have excitation energy between $\varepsilon_2(q)$ and $\varepsilon_1(q)$ in the thermodynamic limit. The $S(q, \omega)$ spectra in the HAF panel of Fig. 9 are for $\alpha = \delta = 0$ and $N = 24$. The color coding is according to the intensity $M_n(q) > 0.001$. There are a few triplets not in class C , but 99.4% of the total intensity is between the dashed lines. The discrete $S(q, \omega)$ spectra are close to the thermodynamic limit for both excitations and intensities.

The $S(q, \omega)$ spectra in the $\alpha = 0.35$ panel of Fig. 9 are for $\delta = 0$, $N = 24$ and color coded according to $M_n(q) > 0.001$. ED returns the full spectrum. The special feature of the triplets shown is greater intensity than over 500 000 other triplets. The triplets account for 99.5% of the total intensity and, again with a few outliers, resemble the spinons in the left panel.

Frustration decreases the dispersion $E_1(q)$ of the lowest triplet, as shown by open circles in the MG ($\alpha = 0.50$) curve. The HAF triplets $E_1(q, N)$ are slightly above $\varepsilon_1(q)$, which at $q = \pi$ is entirely due to finite size. The $q = \pi$, $\alpha = 0.35$ gap is mainly due to finite size while the $\alpha = 0.50$ gap is close to the thermodynamic limit of 0.233 in Fig. 7. The HAF dispersion has previously been used to infer $J_1 = 2E_1/\pi$ from the measured $E_1(\pi/2)$.

Arai *et al.* [37] reported the $S(q, \omega)$ spectrum of CuGeO₃ and interpreted it using the HAF while also pointing out differences. At 10 K, the observed $S(q, \omega)$ intensity peaks at $\pi/2$ and $3\pi/2$ are at 16 meV (186 K). The peaks for $\alpha = 0.35$, $N = 24$ in Fig. 9 are at reduced energy $E_1(\pi/2) = 1.14$, or $E_1 = 182$ K for $J_1 = 160$ K. The agreement is well within the combined accuracy. The $N = 16, 20$, and 24 gaps extrapolated as $1/N$ return $E_1 = 1.1$ in the thermodynamic limit. The weak size dependence is typical of large gaps. The upper limit of the INS spectrum extends [37] to 32 meV at $q = \pi$ at both 10 and 50 K. The calculated $T = 0$ spectrum with appreciable $M_n(\pi)$ also extends to $\omega \sim 2E_1(\pi/2) = 2.28$.

The calculations in Fig. 9 approximate the unknown $S(q, \omega)$ at $\alpha = 0.35$ in the same sense that $N = 24$ approximates the HAF spectrum. $S(q, \omega)$ at $q = \pi/2$ or $3\pi/2$ of CuGeO₃ has a noticeably narrower [37] energy spread than the spinon spread $\varepsilon_2(\pi/2) - \varepsilon_1(\pi/2)$. The correlated states in Fig. 9 capture this narrowing at $\alpha = 0.35$ compared to $\alpha = 0$. Indeed, the width is entirely suppressed at $\alpha = 0.50$, where INS at $q = \pi/2$ or $3\pi/2$ is a δ function at $E = J_1$. This exact result for a triplet, not reported previously, is derived in the Appendix.

The INS data in Fig. 10, upper panel, for the static structure factor $S(T, q)$ of CuGeO₃ is the rescaled Fig. 2 of Ref. [37]. Large differences from HAF were noted [37]. The dashed line is the exact $S(q) = (1 - \cos q)/4$ at $T = \delta = 0$, $\alpha = 0.50$, where finite size simply leads to discrete q . Although $S(q)$ depends on α and δ , the area $\pi/2$ under $S(q)$ does not. The 10 K data are almost as broad as the MG curve before considering the resolution in q .

The calculated $S(T, q)$ in the lower panel of Fig. 10 are for the HAF and for CuGeO₃ parameters: $J_1 = 160$ K, $\alpha = 0.35$, and $T_{SP} = 14$ K. The HAF structure factor for $N = 24$, $\delta = 0$ is strongly peaked at $q = \pi$ and diverges in the thermodynamic limit, but the size dependence elsewhere is small since the area is conserved [38]. The $\alpha = 0.35$ curves at $T = 0$ and 20 K (0.125) are for $N = 24$ and $\delta = 0.025$ and 0, respectively. We obtained explicitly the T dependence of the spin correlation functions in $S(q)$. The $T = 0$ and 20 K

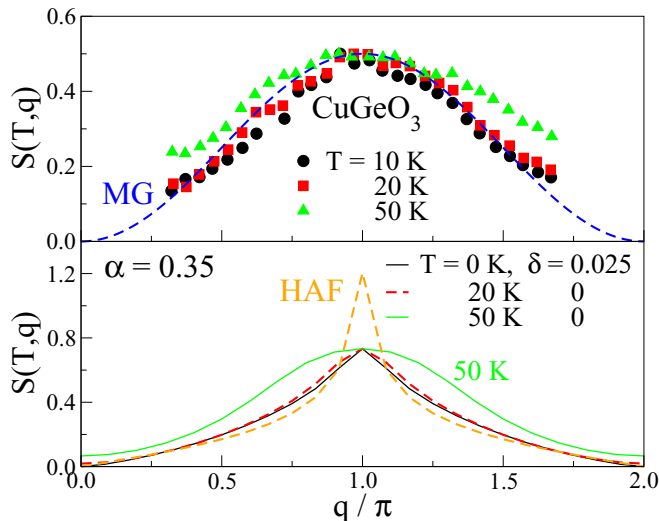


FIG. 10. Upper panel: Static structure factor $S(T, q)$ rescaled from Fig. 2 of Ref. [37]. The exact $S(q)$ at the MG point is $(1 - \cos q)/4$ at $T = 0$. Lower panel: Calculated $S(T, q)$ for $N = 24$ spins at $\alpha = 0.35$ and 0.0 . The area under $T = 0$ curves is $\pi/2$ in both panels. The HAF peak at $q = \pi$ diverges in the thermodynamic limit.

curves illustrate similar spin correlations at $\delta > 0$, $T = 0$ and $T > 0$, $\delta = 0$, as seen in experiment. Convolution with a broadening function in q will be needed to match the observed peaks that depend on resolution in q . The $T = 50$ K (0.313) line is based on $\delta = 0$, $N = 20$ since the thermodynamic limit is reached at lower T . We understand the modest broadening at 50 K by noting that $J_1 = 160$ K is large. We conclude that a 1D model with correlated states accounts reasonably well for these INS data.

V. DISCUSSION

Structural changes at Peierls or SP transitions as well as thermal expansion or contraction have been probed by elastic x-ray or neutron scattering, as discussed in reviews of widely different classes of quasi-1D crystals [39–41]. We note that 3D changes are always found that in some cases exceed those of the 1D chain. While delicate growth conditions leave open the definitive CuGeO_3 structure, the largest change below T_{SP} is along the b axis rather than the $\sim 1\%$ dimerization of the chain along the c axis [42]. Small displacement $\pm u$ of Cu ions along c is consistent with the small calculated $\delta(0) = 0.025$ in the correlated model; they are related by the linear spin-phonon coupling constant. Elastic scattering below T_{SP} from superlattice points is due to structural changes, not just dimerization, that are all initiated at T_{SP} but do not necessarily vary identically with T . Elastic superlattice scattering and coupling to 3D lattices are beyond the scope of this paper.

We have applied the hybrid ED/DMRG method to the best characterized SP transitions and to the J_1 - J_2 model, Eq. (4), with frustration $0 \leq \alpha \leq 0.50$ and isotropic exchange $J_1, J_2 = \alpha J_1$ between first and second neighbors. We exploit the fact that $\delta(0)$ limits the range of spin correlations at $T = 0$ while finite T limits the range at $\delta = 0$. Internal consistency requires T_{SP} to govern both the stiffness $1/\varepsilon_d$ and dimerization $\delta(T)$. The relevant system size depends on T_{SP}/J_1 , about 50

spins for the transitions modeled. When the thermodynamic limit can be reached, the SP transition becomes essentially model exact. On the other hand, the SP instability at $T \sim 0$ is mathematically motivated and beyond the hybrid method. The *general* problem is the SP transition at arbitrary T_{SP} while we have modeled *specific* systems with known T_{SP} .

Correlated states account quantitatively for the magnetic susceptibility of both crystals. On the theoretical side, $\delta(T)$ of that HAF deviates from free fermions or BCS, contrary to previous expectations based on mean field. We place CuGeO_3 in the dimer phase with $\alpha = 0.35$ on the basis of $\chi(T)$, the specific heat, the ratio $\Delta(T)/\Delta(0)$ of the singlet-triplet gap, and INS data that provide an independent determination of $J_1 = 160$ K. The first inorganic SP system is also, to the best of our knowledge, the first physical realization of the dimer phase of the J_1 - J_2 model.

Isotropic exchange between near neighbors is the dominant magnetic interaction that governs the thermodynamics of spin chains. However, such 1D models are approximate and incomplete. Approximate because spin-orbit coupling generates corrections to isotropic exchange and g factors that are more important in Cu(II) systems than for organic radicals. Incomplete because dipolar interaction between spins are neglected, as well as hyperfine interactions with nuclear spins and all interchain interactions. More detailed analysis of specific quasi-1D systems beyond, for example, the J_1 - J_2 model will certainly be needed at low T . Neutron [27–30] and ESR [43] data indicate $J' \sim J_1/10$ between chains and corrections to isotropic exchange, respectively, in CuGeO_3 . The present results establish that the J_1 - J_2 model is the proper starting point for finer low- T modeling.

A static magnetic field H can readily be added to Eq. (4) as $-g\mu_B H S^Z$, where S^Z is the total spin component along H and μ_B is the Bohr magneton. Since total S is conserved, the energy spectrum $\{E(\delta, N)\}$ of correlated states has resolved Zeeman energies when $H > 0$, and the tensor g may often be taken as a scalar. Multiple studies of the SP transition of CuGeO_3 in applied fields of a few teslas have been reviewed [4]. The field dependence has been successfully modeled. We anticipate at most minor changes on analyzing magnetic field effects using correlated states.

We are computing correlation functions of spin- $\frac{1}{2}$ chains as functions of T and H and separation between spins. One goal is to quantify $S(T, q)$, the T dependence of the static structure factor, Eq. (12), in models with increasing frustration α . A limitation of the hybrid method became apparent in connection with $S(q, \omega)$. While ED is computed in sectors with fixed q and S^Z , DMRG is performed in sectors with fixed S^Z up to a cutoff $E_C(\delta, N)$. We can infer S and q , but the $S^Z = 1$ states below the cutoff cluster around $q \sim \pi$ in Fig. 9. The spectrum around $q \sim \pi/2$ that starts at $E > 1$ is soon above $E_C(\delta, N)$ with increasing system size.

In summary, we have modeled the SP transition of the HAF and J_1 - J_2 model with $\alpha \leq 0.5$ in Eq. (4) using correlated states. The thermodynamic limit of finite chains is reached under conditions that are satisfied by TTF- $\text{CuS}_4\text{C}_4(\text{CF}_3)_4$ and CuGeO_3 . The SP transition depends strongly on frustration $\alpha = J_2/J_1$ because the $\alpha < \alpha_c = 0.2214$ phase is gapless with a nondegenerate ground state while $\alpha > \alpha_c$ is gapped with a doubly degenerate ground state.

ACKNOWLEDGMENTS

We thank T. Lorenz for providing us the $\chi(T)$ data. Z.G.S. thanks D. Huse for several clarifying discussions. S.K.S. thanks DST-INSPIRE for financial support. M.K. thanks DST India for financial support through a Ramanujan fellowship.

APPENDIX

Choose the Kekulé diagram with $N/2$ singlet pairs at sites $2r, 2r - 1$ as the ground state $|G\rangle$ at the MG point. The J_1 - J_2 model reads

$$H\left(\frac{1}{2}, 0\right) = H_0 + \sum_{r=1}^{N/2} \left[\vec{S}_{2r} \cdot \vec{S}_{2r+1} + \frac{1}{2} (\vec{S}_{2r-1} \cdot \vec{S}_{2r+1} + \vec{S}_{2r} \cdot \vec{S}_{2r+2}) \right]. \quad (\text{A1})$$

H_0 describes isolated dimers $2r, 2r - 1$ with singlet-triplet gap $E = 1$. The second term acts on adjacent singlets pairs in $|G\rangle$. Direct multiplication of spin functions shows that each term annihilates $|G\rangle$; $E_0 = -3N/8$ is exact.

Let $|2m, 2m - 1\rangle$ be the product function with a triplet at sites $2m, 2m - 1$ and singlets at sites $2r, 2r - 1, r \neq m$. The triplet degeneracy under H_0 is $N/2$. The second term still annihilates $|2m, 2m - 1\rangle$ when acting on adjacent singlets, but not when acting on the triplet and either adjacent singlet. Annihilation requires an out-of-phase linear combination of triplets that occurs at $q = \pi/2$ or $3\pi/2$,

$$|T, \pi/2\rangle = \left(\frac{2}{N}\right)^{\frac{1}{2}} \sum_{m=1}^{N/2} (-1)^m |2m, 2m - 1\rangle. \quad (\text{A2})$$

The normalized triplet $|T, \pi/2\rangle$ is an exact excited state in the thermodynamic limit. In Eq. (11), we find that $S_{\pi/2}^Z |G\rangle = (1/2)|T, \pi/2\rangle$. All INS intensity at $q = \pi/2$ or $3\pi/2$ is at $E = 1$. The other Kekulé diagram with singlet pairs $2r, 2r + 1$ gives the same result.

-
- [1] I. S. Jacobs, J. W. Bray, H. R. Hart, L. V. Interrante, J. S. Kasper, G. D. Watkins, D. E. Prober, and J. C. Bonner, *Phys. Rev. B* **14**, 3036 (1976).
- [2] M. Hase, I. Terasaki, and K. Uchinokura, *Phys. Rev. Lett.* **70**, 3651 (1993); M. Hase, I. Terasaki, K. Uchinokura, M. Tokunaga, N. Miura, and H. Obara, *Phys. Rev. B* **48**, 9616 (1993).
- [3] J. Riera and A. Dobry, *Phys. Rev. B* **51**, 16098 (1995).
- [4] K. Uchinokura, *J. Phys.: Condens. Matter* **14**, R195 (2002).
- [5] S. K. Saha, D. Dey, M. Kumar, and Z. G. Soos, *Phys. Rev. B* **99**, 195144 (2019).
- [6] J. C. Bonner and M. E. Fisher, *Phys. Rev.* **135**, A640 (1964).
- [7] W. P. Su, J. R. Schrieffer, and A. J. Heeger, *Phys. Rev. B* **22**, 2099 (1980).
- [8] G. Beni and P. Pincus, *J. Chem. Phys.* **57**, 3531 (1972).
- [9] L. Del Freo, A. Painelli, and Z. G. Soos, *Phys. Rev. Lett.* **89**, 027402 (2002).
- [10] T. Barnes, J. Riera, and D. A. Tennant, *Phys. Rev. B* **59**, 11384 (1999).
- [11] D. C. Johnston, R. K. Kremer, M. Troyer, X. Wang, A. Klümper, S. L. Bud'ko, A. F. Panchula, and P. C. Canfield, *Phys. Rev. B* **61**, 9558 (2000).
- [12] M. Kumar, S. Ramasesha, D. Sen, and Z. G. Soos, *Phys. Rev. B* **75**, 052404 (2007).
- [13] J. W. Bray, L. V. Interrante, I. S. Jacobs, and J. C. Bonner, in *Extended Linear Chain Compounds*, edited by J. S. Miller (Plenum Press, New York, 1983), Vol. 3, pp. 353–416.
- [14] C. K. Majumdar and D. K. Ghosh, *J. Math. Phys.* **10**, 1399 (1969).
- [15] K. Okamoto and K. Nomura, *Phys. Lett. A* **169**, 433 (1992).
- [16] D. Dey, D. Maiti, and M. Kumar, *Papers Phys.* **8**, 080006 (2016).
- [17] S. K. Saha, M. Kumar, and Z. G. Soos, [arXiv:1907.03724](https://arxiv.org/abs/1907.03724).
- [18] M. Kumar, S. Ramasesha, and Z. G. Soos, *Phys. Rev. B* **81**, 054413 (2010).
- [19] M. C. Cross and D. S. Fisher, *Phys. Rev. B* **19**, 402 (1979).
- [20] K. Fabricius, A. Klümper, U. Löw, B. Büchner, T. Lorenz, G. Dhalenne, and A. Revcolevschi, *Phys. Rev. B* **57**, 1102 (1998).
- [21] M. Hidaka, M. Hatae, I. Yamada, M. Nishi, and J. Akimitsu, *J. Phys.: Condens. Matter* **9**, 809 (1997).
- [22] G. Castilla, S. Chakravarty, and V. J. Emery, *Phys. Rev. Lett.* **75**, 1823 (1995).
- [23] G. Bouzerar, O. Legeza, and T. Ziman, *Phys. Rev. B* **60**, 15278 (1999).
- [24] T. Lorenz, U. Ammerahl, R. Ziemes, B. Büchner, A. Revcolevschi, and G. Dhalenne, *Phys. Rev. B* **54**, R15610 (1996).
- [25] X. Liu, J. Wosnitzer, H. Löhneysen, and R. Kremer, *Z. Phys. B* **98**, 163 (1995).
- [26] T. Wei, A. J. Heeger, M. B. Salamon, and G. E. Delker, *Solid State Commun.* **21**, 595 (1977).
- [27] M. Nishi, O. Fujita, and J. Akimitsu, *Phys. Rev. B* **50**, 6508 (1994).
- [28] J.-G. Lussier, S. M. Coad, D. F. McMorrow, and D. M. Paul, *J. Phys.: Condens. Matter* **8**, L59 (1996).
- [29] M. C. Martin, G. Shirane, Y. Fujii, M. Nishi, O. Fujita, J. Akimitsu, M. Hase, and K. Uchinokura, *Phys. Rev. B* **53**, R14713 (1996).
- [30] L. P. Regnault, M. Aïn, B. Hennion, G. Dhalenne, and A. Revcolevschi, *Phys. Rev. B* **53**, 5579 (1996).
- [31] G. Müller, H. Thomas, H. Beck, and J. C. Bonner, *Phys. Rev. B* **24**, 1429 (1981).
- [32] H. Bethe, *Z. Phys.* **71**, 205 (1931). L. Hulthén, *Ark. Mat. Astron. Fys.* **26**, 106 (1938).
- [33] L. Faddeev and L. Takhtajan, *Phys. Lett. A* **85**, 375 (1981).
- [34] J. des Cloizeaux and J. J. Pearson, *Phys. Rev.* **128**, 2131 (1962).
- [35] M. Karbach, G. Müller, A. H. Bougourzi, A. Fledderjohann, and K.-H. Mütter, *Phys. Rev. B* **55**, 12510 (1997).
- [36] M. Mourigal, M. Enderle, A. Klöpperpieper, J.-S. Caux, A. Stunault, and H. M. Rønnow, *Nat. Phys.* **9**, 435 (2013).

- [37] M. Arai, M. Fujita, M. Motokawa, J. Akimitsu, and S. M. Bennington, *Phys. Rev. Lett.* **77**, 3649 (1996).
- [38] M. Kumar, A. Parvej, and Z. G. Soos, *J. Phys.: Condens. Matter* **27**, 316001 (2015).
- [39] D. Jérôme, *Chem. Rev.* **104**, 5565 (2004).
- [40] J.-P. Pouget, P. Foury-Leylekian, and M. Almeida, *Magnetochemistry* **3**, 13 (2017).
- [41] *Crystals* **7** (2017), special issue on “The Neutral-Ionic Phase Transition”, edited by A. Painelli and A. Girlando.
- [42] Q. J. Harris, Q. Feng, R. J. Birgeneau, K. Hirota, K. Kakurai, J. E. Lorenzo, G. Shirane, M. Hase, K. Uchinokura, H. Kojima, I. Tanaka, and Y. Shibuya, *Phys. Rev. B* **50**, 12606 (1994).
- [43] M. Honda, T. Shibata, K. Kindo, S. Sugai, T. Takeuchi, and H. Hori, *J. Phys. Soc. Jpn.* **65**, 691 (1996).